

Aerodynamic and Structural Design of the Composite Propeller for Near Space Vehicles

Jun Jiao¹, Xiaoping Ma¹, Bifeng Song², Junbo Yang³

¹Institute of Engineering Thermophysics, Chinese Academy of Sciences, Beijing 100190, China

²Department of Aeronautics, Northwestern Polytechnical University, Xi'an 710012, China

³The 38th Research Institute of China Electronic Technology Group Corporation, Hefei 230088, China

Abstract

In order to make full use of the power of engine and reduce the energy consumption, propeller need to be highly efficient and lightweight to satisfy the High Altitude Airship's (HAA) requirements during the high altitude and long endurance flight period. This paper presents an efficient aerodynamic and structural design procedure of the propeller for HAA. First, according to the operating conditions of a HAA's propulsion system, the chord and twist distribution of the propeller blade are optimized to provide the maximum efficiency by GA optimization and propeller vortex theory. Next, the finite element parametric model for the blade is established. Then, based on the aerodynamic characteristics of each blade element, the pressure distribution of blade is calculated by XFOIL, and loaded into the finite element model to investigate the strength of the composite blade. After that, the detailed ply layup and the weight of the blade are obtained by the structural optimal design. The aerodynamic and structural design results show that, compared to the initial blade, the efficiency of the optimized blades which exhibit more mass saving is increased.

Keywords: Propeller, High altitude, Vortex theory, Optimization design

1. Introduction

The ability of high altitude airship to operate for an extended duration of time (months to years) at high altitudes requires a renewable based power system with an efficient propulsion system [1,2]. Therefore, in order to take full advantage of the driven motor power and reduce energy consumption, the propeller systems need to be highly efficient and lightweight. In addition, the propeller efficiency and weight are the basic inputs of the power and energy system, thus the fast and reasonable method for propeller aerodynamic and structural design plays an indispensable role in the overall design of HAA [3,4]. There are two main methods for the aerodynamic and structural design of high altitude propellers. One is the simple approach of applying the blade-element models to propeller aerodynamic design, and using surface area to evaluate the blade weight [5,6], this method is efficient but not particularly accurate. The other is the highly accurate way of combining Computational Fluid Dynamics (CFD) with Finite Element Analysis (FEA) to the composite propeller design [7], however, the calculation is time consuming, and therefore not conducive to the optimization.

In this study, a Genetic Algorithm (GA) based the vortex theory and FEA procedure is developed for aerodynamic and structural design of high altitude propellers. The optimization design procedure by two steps are shown in Figure 1. First, the design variables including chord length and pitch angle of the propeller are determined by GA optimization and propeller vortex theory. Next, the full finite element parametric model of the optimized propeller blade is established. Then, based on the aerodynamic characteristics of each blade element, the pressure distribution of propeller blade is calculated by XFOIL, and loaded into the finite element model to investigate the strength of the composite blade. After that, the detailed ply layup and the weight of the blade are obtained by the structural optimal design.

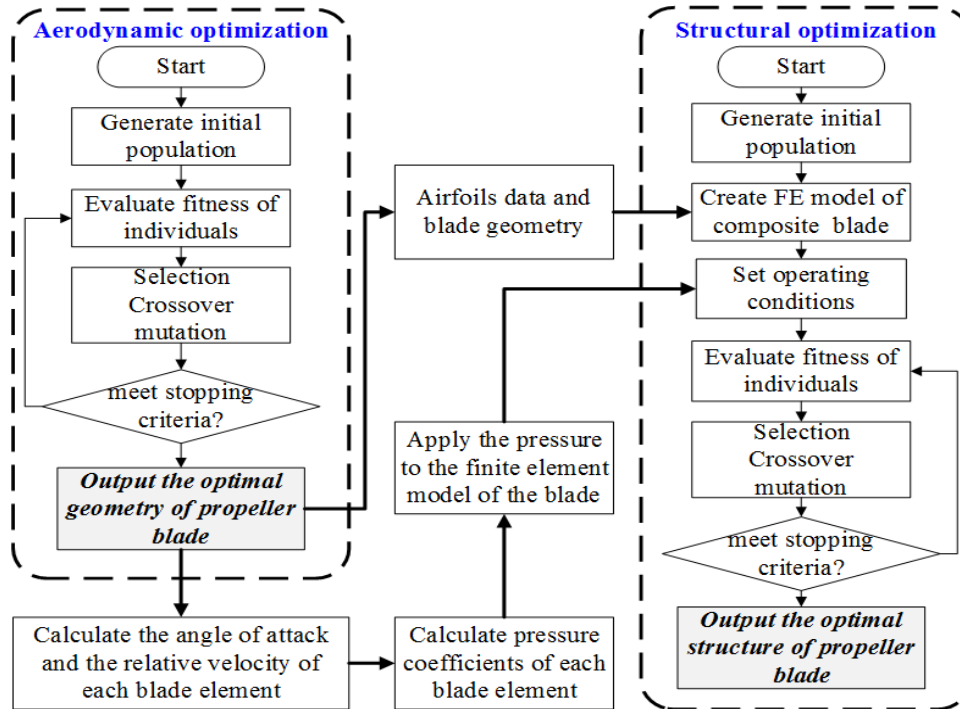


Figure 1 – Aerodynamic and structural design procedure of a composite propeller

2. Aerodynamic design of high altitude propeller

2.1 Vortex theory of propeller

In order to quantitatively predict the performance of a rotating propeller, the aerodynamics of the blade need to be analyzed in detail. To this end, the cross-section of the propeller blade is shown in Figure 2. The aerodynamic performance including thrust T , torque M , and efficiency η , etc., of propeller would be iteratively computed when the geometry and operating condition of the blade are determined [8,9].

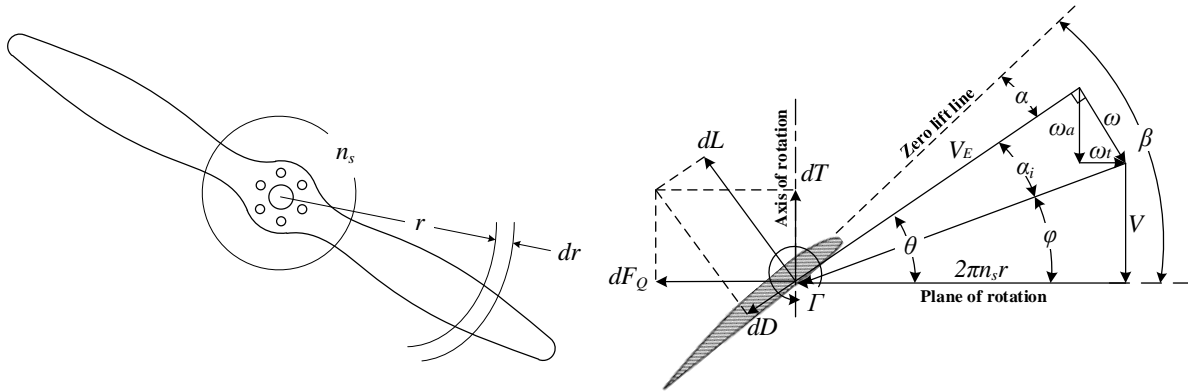


Figure 2 – Section forces and velocities acting on a rotating propeller blade

The propeller is rotating with a rotational speed of n_s and advancing through the air with velocity of V . The pitch angle, β , is defined relative to the zero lift line of the airfoil section which varies with the radial distance r . Similar to finite wing theory, the total down wash angle, θ , is the sum of two parts, the advanced angle, ϕ , and induced angle of attack resulting from the induced velocity ω , α_i , the contribution of one-blade element to the thrust, dT , and torque, dQ , are related to the differential lift and drag forces.

$$dT = \frac{1}{2} \rho V_E^2 c [C_l \cos(\phi + \alpha_i) - C_d \sin(\phi + \alpha_i)] dr \quad (1)$$

$$dQ = \frac{1}{2} \rho V_E^2 c [C_l \sin(\phi + \alpha_i) + C_d \cos(\phi + \alpha_i)] r dr \quad (2)$$

The section lift and drag coefficient, C_l and C_d , depend on the local Reynolds and Mach number, Re and Ma , and aerodynamic angle of attack for the blade element, α . From the tangential and axial

component of induced velocity, ω_t and ω_a , the angle of attack α be determined as

$$\alpha = \beta - \varphi - \alpha_i = \beta - \theta = \beta - \tan^{-1} \left(\frac{V + \omega_a}{2\pi n_s r - \omega_t} \right) \quad (3)$$

And the induced angle can also be determined easily from the same geometry as

$$\alpha_i = \theta - \varphi = \tan^{-1} \left(\frac{V + \omega_a}{2\pi n_s r - \omega_t} \right) - \tan^{-1} \left(\frac{V}{2\pi n_s r} \right) \quad (4)$$

The resultant relative velocity, V_E , at the plane of the blade is given by

$$V_E = \sqrt{(V + \omega_a)^2 + (2\pi n_s r - \omega_t)^2} \quad (5)$$

The Kutta-Joukowski theorem states that the lift on a finite propeller blade is related to the bound vorticity through the vortex lifting law. Thus, the local section circulation, Γ , can be expressed as

$$\Gamma = \frac{1}{2} c C_l V_E \quad (6)$$

According to Goldstein's vortex theory, the induced velocity is assumed to be normal to the resultant velocity, thus the two parts of the induced velocity are related by

$$\frac{V + \omega_a}{2\pi n_s r - \omega_t} = \frac{\omega_t}{\omega_a} \quad (7)$$

Goldstein's vortex theory relates the local tangential component of induced velocity, ω_t , to the bound circulation, Γ , around any blade section by

$$B\Gamma = 4\pi r \kappa \omega_t \approx 4\pi r F \omega_t \quad (8)$$

The Goldstein's kappa factor, κ , which is difficult to find a numerical solution, is replaced by Prandtl's tip loss factor, F . It is expressed as

$$F = \frac{2}{\pi} \cos^{-1} \left\{ \exp \left[-\frac{B(1 - 2r/d)}{2 \sin \beta_t} \right] \right\} \quad (9)$$

where d is the diameter of the propeller, B is the number of blades and β_t is the pitch angle at the propeller blade tip.

2.2 The aerodynamic optimization model

2.2.1 The Objective Function

The ability of airships to operate for an extended duration of time (months to years) at high altitudes requires a renewable based power system with an efficient propulsion system. Therefore, in order to take full advantage of the driven motor power and reduce energy consumption, the propeller systems of HAA need to be highly efficient. Therefore, the minimum mass for the propeller blade is taken as the objective function.

$$\text{Objective: } f(x) = \max(\eta) \quad (10)$$

2.2.2 Design Variables and Constraints

The propeller blade geometry and operating conditions determine the aerodynamic efficiency of the propeller. In addition to the cross-sectional airfoil, the geometry of the propeller blade are mainly determined by distribution of chord and pitch angle. In order to make the blade shape smooth and continuous along the spanwise direction, the cubic Bézier curve [10] is used to describe the blade chord and the pitch angle distribution.

$$c(x) = (1-x)^3 c_0 + 3x(1-x)^2 c_1 + 3x^2(1-x) c_2 + x^3 c_3 \quad (11)$$

$$\beta(y) = (1-y)^3 \beta_0 + 3y(1-y)^2 \beta_1 + 3y^2(1-y) \beta_2 + y^3 \beta_3 \quad (12)$$

where c_0, c_1, c_2 and c_3 represent four control points of the chord distribution, one at hub, one at tip and two at intermediate stations, $\beta_0, \beta_1, \beta_2$ and β_3 represents the control points of the pitch angel distribution, x, y changes in $[0, 1]$, the range of eight parameters is limited as follows,

$$c_{i\min} \leq c_i \leq c_{i\max} \quad \beta_{i\min} \leq \beta_i \leq \beta_{i\max} \quad i=0,1,2,3 \quad (13)$$

In addition, in order to take into account the performance of the drive motor, the range of values for rotational speed should be subject to a reasonable limitation as a design variable. Thus, the design variables and their bounds are described in Table 1.

$$\text{Design variables: } c_0, c_1, c_2, c_3, \beta_0, \beta_1, \beta_2, \beta_3, n_s \tag{14}$$

Table 1 – Aerodynamic design variables and their ranges

Variable	Description	Range
c_0		0.1~0.6
c_1	The control parameters	0.2~1.0
c_2	of chord distribution, m	0.2~1.0
c_3		0.1~0.6
β_0		20~60
β_1	The control parameters of	20~60
β_2	pitch angle distribution, degree	1~30
β_3		1~30
d	Propeller's diameter, m	6.8
n_s	Propeller's rotational speed, rpm	500~600
B	Number of blades	2

The required thrust under the flight condition and the rated power absorbed from the motor are both restricted based on the task requirement and propulsion system of HAA. Because the rotational speed are both changing during the design process, the tip Mach number of the propeller must be limited lower than 0.7 Mach which can be achieved easily under high altitude and low density environment [11]. This is done to avoid the formation of shock waves over the surface of the blade which can severely reduce its performance if not destroy the propeller.

$$\text{Constraints: } T \geq 90\text{kgf}, P_{\text{shaft}} \leq 25.5\text{kW}, Ma_{\text{tip}} \leq 0.7 \tag{15}$$

2.3 Aerodynamic Optimization results

The original two-bladed propeller with 6.8-meter diameter operating at 20km altitude for a HAA is optimized in this part. Figure 3 shows the comparison of blade geometry and aerodynamic performance between the initial and optimized propeller. It is seen that the optimized propeller has a higher aerodynamic efficiency than the initial one at every advance ratios. The efficiency of the optimized propeller is about 69% at the design point, and is increased by 2% compared with the original scheme.

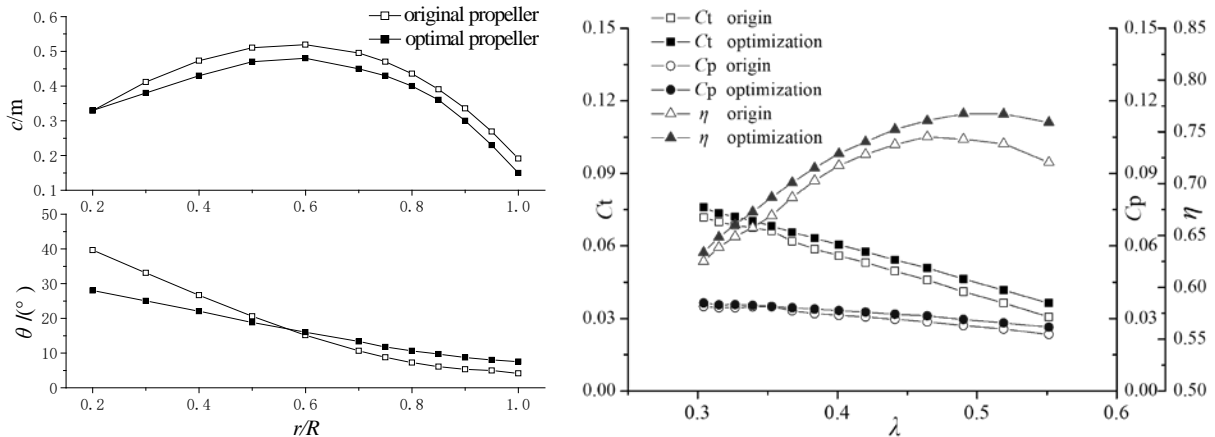


Figure 3 – Comparison of shape and performance between the original and optimized propeller

3. Structural design of the composite propeller

3.1 Parametric finite element model of propeller blade

This part focused on the structural design of the 6.8m high altitude propeller blade. A two shear web design is chosen in the blade section. Figure 4 shows that the webs divide the blade section into three parts. The outer surface of the blade is a skin which is used to construct a blade with complex geometry.

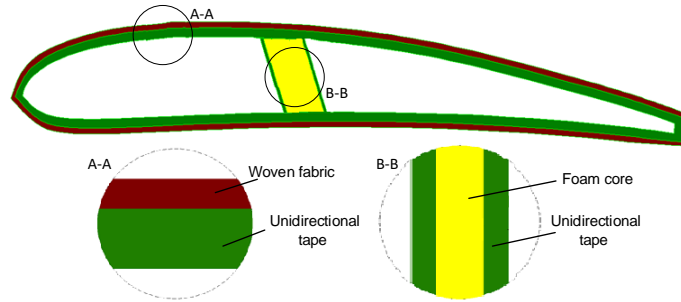


Figure 4 – Material of blade section

For the composite propeller blade, the prepregs used were T700 unidirectional tape and G814 woven fabric reinforced by epoxy resin. Table 1 lists the elastic property data for the materials chosen for this design.

Table 2 – Mechanical properties of composite blade

Material	E_1 (GPa)	E_2 (GPa)	Poisson's ratio	G_{12} (GPa)	Density(kg/m ³)
T700/epoxy	120	8	0.25	4.5	1600
G814/3234	70	70	0.062	4.1	1650
Foam core	0.07	0.07	0.25	0.019	52

A program of building parametric finite element model of the propeller blade which combined MATLAB and PCL language of PATRAN software is developed. The procedure is as follows.

- (1) Based on the Bézier fitting method of three-dimensional shapes of the blade, the data of the three-dimensional blade geometry is outputted in a certain specific format.
- (2) The initial material properties and layout data were employed to meshing the surface of the blade elements. Thus the layout materials, the thickness of laminates and the angle of plies are defined.
- (3) Write a macro-files using PCL language, which can transfer the data calculated from MATLAB into PATRAN software.
- (4) Create the entire finite element model of propeller blade and obtain the NASTRAN input file, including the blade surface model, boundary conditions, and initial material properties.

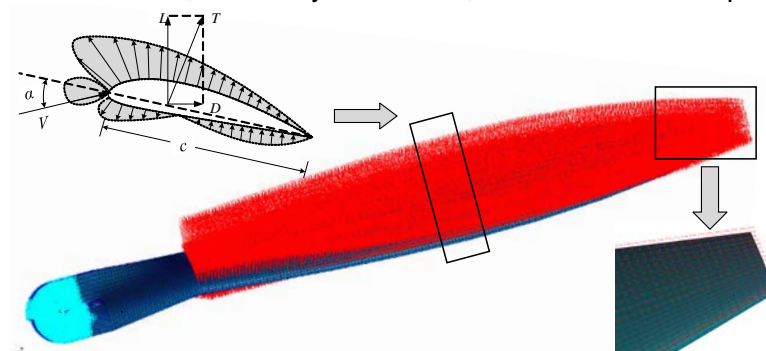


Figure 5 – Interpolation of aerodynamic pressure

Figure 5 illustrates the aerodynamic interpolated method that applied the pressure load to the structural finite element model [12,13]. After determining the operating conditions of the propeller, the pressure coefficients for each blade element could be acquired by XFOIL[14]. The varying

aerodynamic load along the whole blade will be imposed on the corresponding blade elements. Therefore, the pressure distribution for each blade section can be translated into a function with a high order polynomial to be applied to the finite element model. The pressure distributions on the whole blade after interpolating the aerodynamic load is shown in Figure 6.

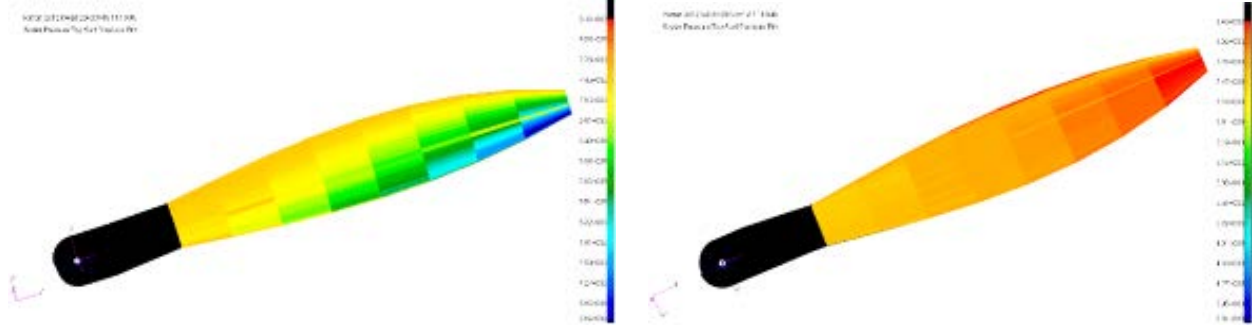


Figure 6 – Pressure distribution of the blade upper and lower surface

3.2 The Structural optimization model

3.2.1 The Objective Function

Figure 7 shows the region division of the composite propeller blade [15]. The blade can be divided into 9 regions from wing root to tip based on the blade element location. The objective is the minimum mass of the composite propeller blade. The upper and lower skins of the blade in same region contain the same laminate configuration stacking in this problem for simplicity.

$$\text{Objective: } f(x) = \min(m) \tag{16}$$

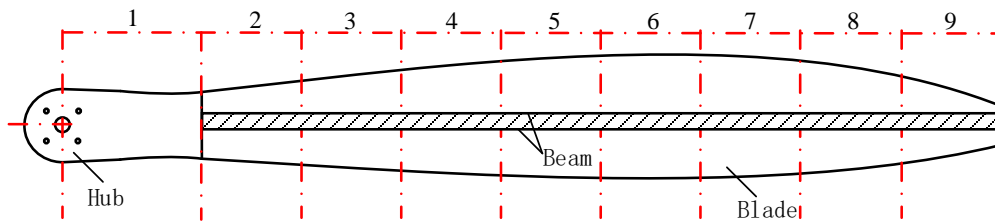


Figure 7 – Region division of the propeller blade

3.2.2 Design Variables and Constraints

This paper applied the guide based design approach proposed by Adams [16] to establish the structural optimization model of the composite blade. The basic laminate stacking sequence (referred as the guide) that is applicable to all the panels is used as a design layout, while the individual local panels use only a segment of the guide starting either from the top or from the bottom of the guide. This ensures complete blending at any stage of the design optimization process.

For a single ply, three different indicators are introduced to incorporate optimization formulations in the design process [17]. The first indicator uses an integer to determine its ply angle: $\theta = 1; 2; 3$, and 4 denotes the fiber angle of 0, 45, -45 and 90 deg. The second indicator uses an integer distance to determine how many regions a ply occupied: $L = 2$ denotes that the ply extends through the first two regions, $L = 0$ denotes that the ply does not exist, etc. The third indicator uses an integer to determine the material type: $M = 1$ denotes that the prepreg of the ply is G814/3234, $M = 2$ denotes that the prepreg of the ply is T700/epoxy. Thus the design variables in the optimization formulation are the three different indicators of every ply.

$$\text{Design variables: } M, \theta, L \text{ of every ply} \tag{17}$$

The lamination parameters of guide laminate and ply number of each panel are adjusted using the Mixed Integer genetic algorithm (MIGA) [18] with structure behavior constraints. The following

describe the design constraints used for the optimization of the composite blade.

(1) Strength constraints are introduced to limit the magnitude of strains in tension, compression, and shear taken by the laminate. This is conducted in terms of allowable strains. Strains in x, y, and xy directions are restrained.

(2) For the stiffness constraints, the propeller tip displacement constraint and twist angle constraint are used to maintain the bending and torsion stiffness of the blade and to prevent the aero loads from being deteriorated.

(3) In order to avoid the resonance during operation, the first order natural frequency of the propeller should be greater than 17Hz.

(4) Because of the damage tolerance requirements, there must exist at least three plies along the whole length of the blade. The number of plies in any one direction placed sequentially in the stack is limited to four.

$$Constraints : RF = \frac{\epsilon^i}{[\epsilon^i]} \leq 1 \quad (i = x, y, xy), DIS \leq 50mm, TA \leq 0.4^\circ, FRE \geq 17Hz \quad (18)$$

3.3 Structural Optimization results

Table 2 details the optimum design of the composite surface obtained by this optimization method.

Table 3 – Stacking sequence of every region after optimization

Regions	Stacking piles	Stacking sequences
1	64	[45 ₂ 0 45 -45 0 0 ₂ -45 0 ₂ -45 0 ₂ 90 0 ₃ 45 0 0 -45 -45 0 ₂ 0 0 -45 90 45 90 0] _s
2	64	[45 ₂ 0 45 -45 0 0 ₂ -45 0 ₂ -45 0 ₂ 90 0 ₃ 45 0 0 -45 -45 0 ₂ 0 0 -45 90 45 90 0] _s
3	54	[45 ₂ 0 45 -45 0 0 ₂ -45 0 ₂ -45 0 ₂ 90 0 ₃ 45 0 0 -45 0 90 45 90 0] _s
4	40	[45 ₂ 0 -45 0 0 ₂ -45 0 ₂ -45 0 ₂ 45 0 -45 90 45 90 0] _s
5	26	[45 ₂ -45 0 0 ₂ 45 0 -45 90 45 90 0] _s
6	18	[45 ₂ -45 0 0 ₂ 45 -45 90] _s
7	14	[45 ₂ -45 0 45 -45 90] _s
8	10	[45 ₂ 0 45 -45] _s
9	8	[45 ₂ 0 45] _s

The structural behaviors of the optimized composite blade which analyzed with the finite element software NASTRAN are shown as follow.

Table 4 – Blade strength, stiffness and frequency

Parameter	Displacement (mm)	Twist angle (°)	Strain (μϵ)			Frequency (Hz)
			x	y	xy	
Value	46	0.38	897	928	979	17.001

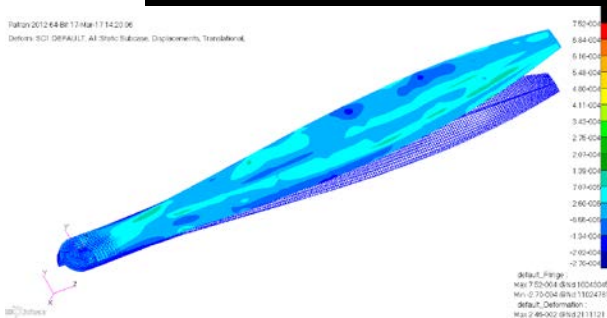


Figure 8 – Strain contour in x direction

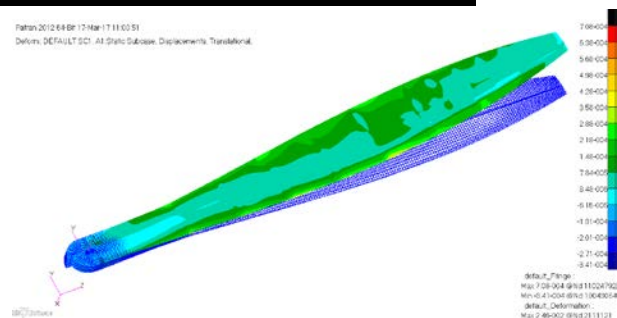


Figure 9 – Strain contour in y direction

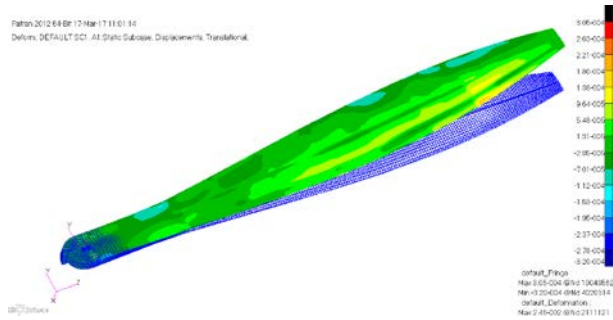


Figure 10 – Strain contour in xy direction

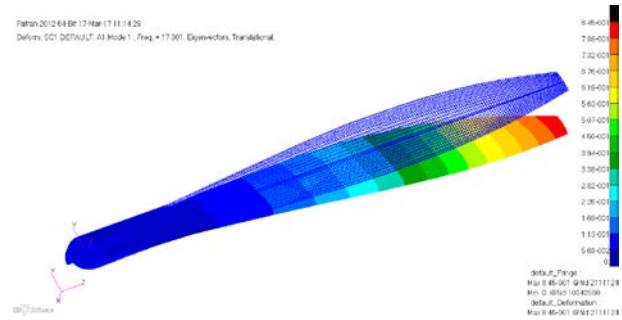


Figure 11 – First order natural frequency

4. Conclusion

In this study, an efficient aerodynamic and structural design procedure is developed for a 6.8m composite propeller of HAA. The geometry of the propeller blade are optimized to provide the maximum efficiency by GA optimization and propeller vortex theory. The efficiency of the optimized propeller is about 69% at the design point, and is increased by 2% compared with the original scheme. The aerodynamic interpolated method that applied the pressure load to the structural finite element model is presented based on the pressure coefficients for each blade element calculated by XFOIL. A parametric element model of the composite propeller blade is built. Coupling FEA program and MIGA algorithm leads to a powerful tool suitable for composite propeller blade optimization.

5. Contact Author Email Address

Jun Jiao: jiaojun@iet.cn

6. Copyright Statement

The authors confirm that they, and/or their company or organization, hold copyright on all of the original material included in this paper. The authors also confirm that they have obtained permission, from the copyright holder of any third party material included in this paper, to publish it as part of their paper. The authors confirm that they give permission, or have obtained permission from the copyright holder of this paper, for the publication and distribution of this paper as part of the ICAS proceedings or as individual off-prints from the proceedings.

References

- [1] Young M, Keith S and Pancotti A. An overview of advanced concepts for near space systems. *45th AIAA/ASME/SAE/ASEE Joint Propulsion Conference & Exhibit*, Denver, Colorado, AIAA 2009-4805, 2009
- [2] Ilieva G, Páscoa J, Dumas A and Trancossi M. A critical review of propulsion concepts for modern airships. *Open Engineering*, Vol. 2, No. 2, pp 189-200, 2012.
- [3] Morgado J, Abdollahzadeh M, Silvestre M A R and Páscoa J C. High altitude propeller design and analysis. *Aerospace Science and Technology*, No. 45, pp 398-407, 2015.
- [4] Colozza A. High altitude propeller design and analysis overview. NASA/CR 98-208520, 1998.
- [5] Liu X, He W and Wei F. Design of high altitude propeller using multilevel optimization. *International Journal of Computational Methods*, Vol. 17, No. 4, pp 1950004-1-32, 2020.
- [6] Jiao J, Song B, Zhang Y and Li Y. Optimal design and experiment of propellers for high altitude airship. *Proceedings of the Institution of Mechanical Engineers - Part G: Journal of Aerospace Engineering*, Vol. 232, No. 10, pp 1887-1902, 2018.
- [7] Bazilevs Y, Hsu M C, Akkerman I, et al. 3D simulation of wind turbine rotors at full scale. *International journal for numerical methods in fluids*, Vol. 65, No. 1-3, pp 207-235, 2011.
- [8] McCormick BW. *Aerodynamics, aeronautics, and flight mechanics*. New York: John Wiley and Sons, 1995.
- [9] Adkins C N, Liebeck R H. Design of optimum propellers. *Journal of Propulsion and Power*, Vol. 10, No. 5, pp 676-682, 1994.
- [10] Benini E, Toffolo A. Optimal design of horizontal-axis wind turbines using blade-element theory and evolutionary computation. *Journal of Solar Energy Engineering*, Vol. 124, No. 4, pp 357-363, 2002.
- [11] Colozza A. APEX 3D propeller test preliminary design. NASA/CR-2002-211866, 2002.
- [12] Chen J, Wang Q, Shen W Z, et al. Structural optimization study of composite wind turbine blade. *Materials & Design*, Vol. 46, pp 247-255, 2013.

AERODYNAMIC AND STRUCTURAL DESIGN OF THE COMPOSITE PROPELLER

- [13] Aceves C M, Sutcliffe M P F, Ashby M F, et al. Design methodology for composite structures: a small low air-speed wind turbine blade case study. *Materials & Design (1980-2015)*, Vol. 36, pp 296-305, 2012.
- [14] Drela M. XFOIL: An analysis and design system for low Reynolds number airfoils. *Low Reynolds number aerodynamics*, Springer Berlin Heidelberg, 1989.
- [15] Meng J, Hu J, Xiao H, et al. Hierarchical optimization of the composite blade of a stratospheric airship propeller based on genetic algorithm. *Structural and Multidisciplinary Optimization*, Vol. 56, No. 6, pp 1341-1352, 2017.
- [16] Adams D B, Watson L T, Gürdal Z and Anderson-Cook C M. Genetic algorithm optimization and blending of composite laminates by locally reducing laminate thickness. *Advances in Engineering Software*, Vol. 35, pp 35-43, 2004.
- [17] Jin P, Song B and Zhong X. Structure optimization of large composite wing box with parallel genetic algorithm. *Journal of aircraft*, Vol. 48, No. 6, pp 2145-2148, 2011.
- [18] Deep K, Singh K P, Kansal M L, et al. A real coded genetic algorithm for solving integer and mixed integer optimization problems. *Applied Mathematics and Computation*, Vol. 212, No. 2, pp 505-518, 2009.